Periodicity of the Lorenz–Stenflo equations

2015 Phys. Scr. 90 065201

(http://iopscience.iop.org/1402-4896/90/6/065201)

IOP Publishing | Royal Swedish Academy of Sciences Physica Scripta

Phys. Scr. **90** (2015) 065201 (5pp) doi:10.1088/0031-8949/90/6/065201

Periodicity of the Lorenz–Stenflo equations

Junho Park[1,3], Hyunho Lee[1], Ye-Lim Jeon[2] and Jong-Jin Baik[1]

[1] School of Earth and Environmental Sciences, Seoul National University, Seoul 151-742, Korea
[2] Departement of Earth Science Education, Seoul National University, Seoul 151-742, Korea

E-mail: junho.park@snu.ac.kr, leehh@snu.ac.kr, yelmi0608@snu.ac.kr and jjbaik@snu.ac.kr

Received 9 January 2015
Accepted for publication 5 February 2015
Published 21 April 2015

Abstract

In this paper, we investigate periodic behaviors of the Lorenz–Stenflo equations in wide ranges of parameters. Regimes of periodic solutions and chaotic solutions are computed and distinguished by local maximum values of a dynamic variable Z. Complex behaviors of the periodic solutions are observed inside a regime of the chaotic solutions which is closed and surrounded by a regime of the periodic solutions where a feature of disconnected bifurcations is observed. It is found that not only a regime of fixed solutions but also regimes of solutions with period 1 and 2 remain for sufficiently large parameters.

Keywords: Lorenz–Stenflo equations, periodicity, chaos, nonlinear dynamics

(Some figures may appear in colour only in the online journal)

1. Introduction

The Lorenz–Stenflo equations are nonlinear equations originally derived for atmospheric acoustic-gravity waves by including an effect of the Earth's rotation with the new parameter s and the new dynamic variable V [1]. The Lorenz–Stenflo equations become equivalent to the Lorenz equations as the rotational parameter s becomes zero [1, 2]. After Stenflo [1], dynamics of the Lorenz–Stenflo equations has been widely investigated in the last two decades. Yu and Yang [3] firstly performed a stability analysis on the Lorenz–Stenflo equations and showed that both periodic and chaotic solutions exist in the regime of instability and their behaviors in the parameter r space at $s = 30$ are very similar to those in the Lorenz equations. In the very next paper by Yu *et al* [4], they studied bifurcation characteristics of the Lorenz–Stenflo equations and found that both forward and backward bifurcations exist for s bifurcation space, while only the backward bifurcation is observed in r bifurcation space, of the Lorenz equations. In Zhou *et al* [5], they investigated bifurcation structures and periodic orbits for large s and suggested that there are much richer dynamical behaviors occurring for large s than those of the Lorenz equations. More results on chaos, bifurcations and periodic orbits of the Lorenz–Stenflo equations are also presented in Zhou *et al* [6]. While these papers investigated periodic and chaotic behaviors for a few parameters of s, Xavier and Rech [7] studied the chaotic dynamics in wide ranges of r and s by computing Lyapunov exponents in the r-s parameter space. They found that inside the chaotic regime, there are periodic regimes with a shrimp shape. These shrimp-shape periodic islands are also observed in the Hénon map [8], modulated CO_2 laser [9] or Chua's circuit [10]. But unlike these systems, appearance of these periodic islands in the Lorenz–Stenflo equations is not organized. Moreover, there are not only the shrimps but also long bands, narrow periodic windows, etc.

While the chaotic dynamics is well studied by Xavier and Rech [7], periodic behaviors of the Lorenz–Stenflo equations are not fully investigated, particularly the periodic behaviors for large s which may be regarded as large-scale periodic motions in atmospheric turbulence under a strong effect of the Earth's rotation. In this paper, we investigate the periodic behaviors thoroughly in wide ranges of r and s. Only effects of the parameters r (i.e. effect of the Rayleigh number) and s are investigated and the parameters σ and b are fixed as $\sigma = 10$ and $b = 8/3$ same as Lorenz [2].

2. The Lorenz–Stenflo equations and numerical method

The Lorenz–Stenflo system consists of equations as follows:

$$\dot{X} = \sigma(Y - X) + sV, \tag{1}$$

[3] Author to whom any correspondence should be addressed.

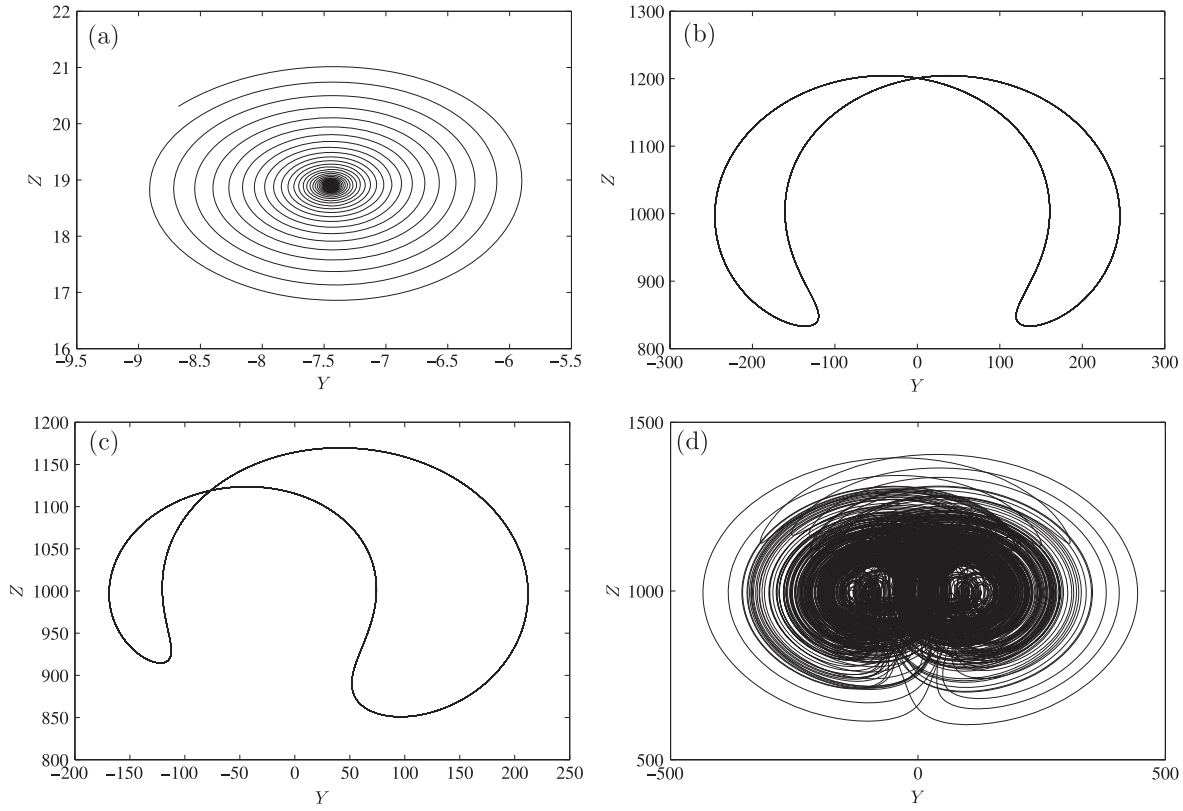

Figure 1. Trajectories on the Y–Z plane for (a) fixed solution ($r = 20$, $s = 10$), (b) period 1 solution ($r = 1000$, $s = 10$), (c) period 2 solution ($r = 1000$, $s = 200$) and (d) chaotic solution ($r = 1000$, $s = 600$). Only for the fixed and chaotic solutions in (a) and (d), initial data from $t = 0$ to $t = 10$ are truncated in order to observe more clearly a spiral pattern converging to the stationary point and a chaotic behavior, respectively.

$$\dot{Y} = rX - XZ - Y, \tag{2}$$

$$\dot{Z} = XY - bZ, \tag{3}$$

$$\dot{V} = -X - \sigma V, \tag{4}$$

where X, Y, Z and V are the dynamical variables, dot denotes the derivative with respect to the time t, σ is the Prandtl number, r is the generalized Rayleigh parameter, b is the geometric parameter, and s is the parameter associated with the Earth's rotation [1, 2]. By applying $\dot{X} = \dot{Y} = \dot{Z} = \dot{V} = 0$, three stationary points of the equations can be obtained as follows:

$$P_o = (0, 0, 0, 0), \; P_{\pm} = \left(\pm X_s, \pm Y_s, Z_s, \pm V_s\right), \tag{5}$$

where $X_s = \sqrt{bZ_s \Big/ \left(1 + s\big/\sigma^2\right)}$, $Y_s = \sqrt{bZ_s(1 + s/\sigma^2)}$, $Z_s = r - 1 - s\big/\sigma^2$ and $V_s = -X_s/\sigma$. Based on the linear stability analysis, the point P_o firstly becomes unstable with the pitchfork bifurcation as r increases, then the points $P_{\pm}$ become unstable with the Hopf bifurcation (for more details on stability properties, refer to Yu and Yang [3] and Xavier and Rech [7]).

For unstable solutions, numerical integrations of equations (1)–(4) are performed using the 4th order Runge–Kutta method with initial conditions $X_0 = 10^{-2}$, $Y_0 = V_0 = 0$ and $Z_0 = r$. The data are truncated from $t = 0$ to $t = 100$ in order to ignore transient behaviors by initial conditions, similar to the data truncation procedure by Yu *et al* [4]. We tested a lot of parameters and confirmed that solutions are on their converged periodic trajectories or chaotic attractors after the truncation. 50000 iterations are then additionally performed after $t = 100$ with a time resolution $\Delta t = 10^{-4}$. The additional iterations with such Δt are sufficient to capture periodicity or chaotic behavior of solutions in the parameter space of our interest. After the time integrations, local maximum values of the variable $Z(t)$ are picked and they are regarded as different maximums if they differ with a relative tolerance more than 0.1%.

3. Numerical results

Figure 1 shows trajectories of solutions on the Y–Z plane. Fixed solutions eventually converge to the stationary points $P_{\pm}$ as displayed in figure 1(a). For non-fixed solutions, we find all maximum values of Z on the trajectories and define periodicity of the solutions as the number of maximum values $Z_{\max}$. For example, in figure 1(b), the variable Z has only one maximum about $Z = 1204$ so the period is 1. Figure 1(c) shows an example of period 2 solution which has two maximums, one about $Z = 1170$ and the other about $Z = 1124$.

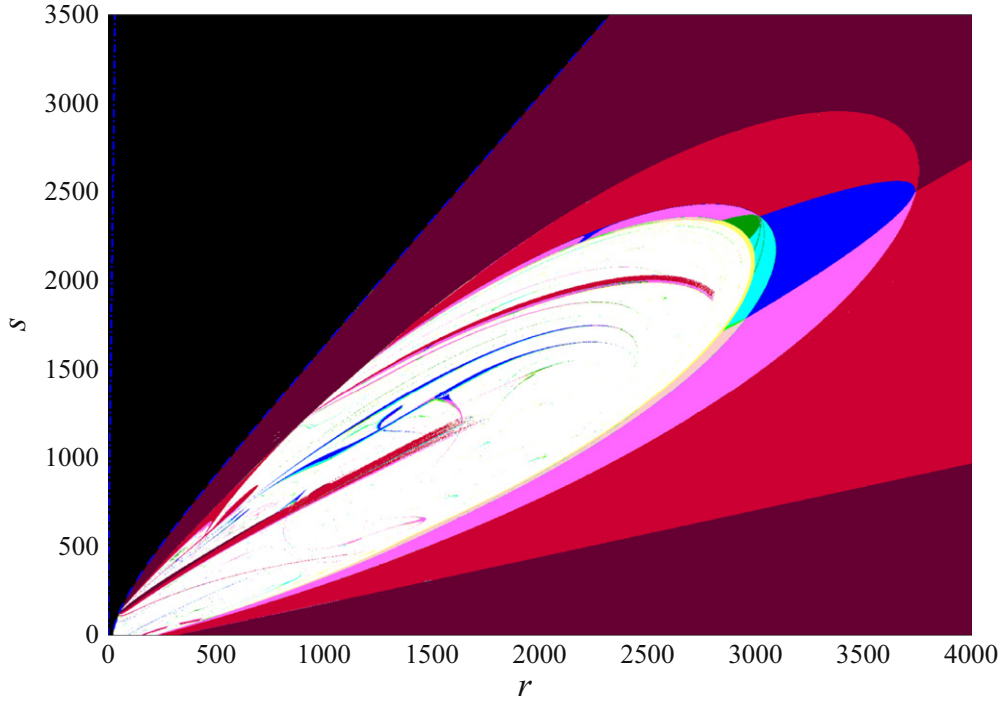

Figure 2. Periodicity diagram in the r–s parameter space for $0 \leqslant r \leqslant 4000$ and $0 \leqslant s \leqslant 3500$. Colors indicate the periodicity of solutions: fixed solutions (black), period 1 (dark red), period 2 (red), period 3 (blue), period 4 (pink), period 5 (green), period 6 (cyan), period 7 (light green), period 8 (light pink), period 9–16 (yellow) and period higher than 16 or chaotic solutions (white). Blue dash-dot and dashed lines represent curves on which the pitchfork bifurcation and the Hopf bifurcation occur, respectively.

Note that while the trajectory with period 1 is symmetric with respect to $Y = 0$, symmetry of the period 2 trajectory is broken (for more details on periodic orbits, refer to Zhou *et al* [5]). Figure 1(d) shows an example of chaotic solutions and we clearly see a chaotic attractor. In fact, the number of maximum values $Z_{\max}$ cannot be decided for the chaotic solutions since it increases as more time integrations are performed.

Following Dullin *et al* [11] who investigated a periodicity diagram of the Lorenz equations in the r-σ parameter space, we obtained a periodicity diagram of the Lorenz–Stenflo equations in the r-s parameter space with resolutions $\Delta r = \Delta s = 1$, as displayed in figure 2. Although these resolutions are not sufficient to capture very narrow periodic windows [6], we fix these values to obtain an extensive diagram to understand the dynamics of the Lorenz–Stenflo equations at a glance. During numerical computations, periodicity of solutions is distinguished from period 1 to 16. There are also solutions with periodicity higher than 16 but these solutions become chaotic immediately and cover very small areas in the parameter space, thus it was difficult to distinguish them from chaotic solutions.

Regime of the fixed solutions colored by black is separated by the blue dashed line which represents the line of the Hopf bifurcation where all the stationary points (5) become linearly unstable. This critical curve $r_{c,H}(s)$ is already well investigated and analytically expressed in [5, 7]. From these papers, we obtain an asymptotic expression for sufficiently large s such that the critical value of $r_{c,H}(s)$ becomes linear at the leading order in the form of $r_{c,H} \sim A_H s$ where

$$A_H = \frac{-B_H + \sqrt{B_H^2 - C_H}}{2b\sigma}, \tag{6}$$

$$B_H = (1 + 2\sigma - b)\left(\frac{1}{\sigma} - 1\right) - \frac{2b}{\sigma}, \tag{7}$$

$$C_H = 4b\left(1 - \frac{2}{\sigma}\right)\left\{\left(\frac{1}{\sigma} - 1\right)(1 + 2\sigma) - \frac{b}{\sigma}\right\}. \tag{8}$$

For $\sigma = 10$, $b = 8/3$, the value of A_H is 0.7188. Similarly for the pitchfork bifurcation indicated by the blue dash-dot line in figure 2, the critical value $r_{c,p}$ is $r_{c,p} = \min\left(1 + s/\sigma^2, 2 + \sigma + s/\sigma\right)$ [7], thus $r_{c,p}$ is also linearly proportional to s.

For $r > r_{c,H}$, there are both chaotic and periodic regimes. There exist immersed regimes of periodic solutions inside the chaotic regime with various shapes such as long curved bands with period 1 and powers of 2 (thick bands with red and pink colors), thin curves of period 3 and 6 solutions with blue and cyan colors, shrimp-shape periodic islands [7], narrow periodic windows displayed as thin dotted lines, etc. All these regimes represent the complexity of the nonlinear Lorenz–Stenflo equations since their appearance is not organized and not predictable.

However, chaotic solutions no longer exist but all solutions become fixed or periodic for $s > 2340$ or for $r > 2975$. To understand this, we apply new scales to the variables following [11, 12], for large r and small ϵ as $t = \epsilon\tau$, $X = \alpha x$, $Y = \beta y$, $Z - r = \zeta z$ and $V = \delta v$, and obtain the following

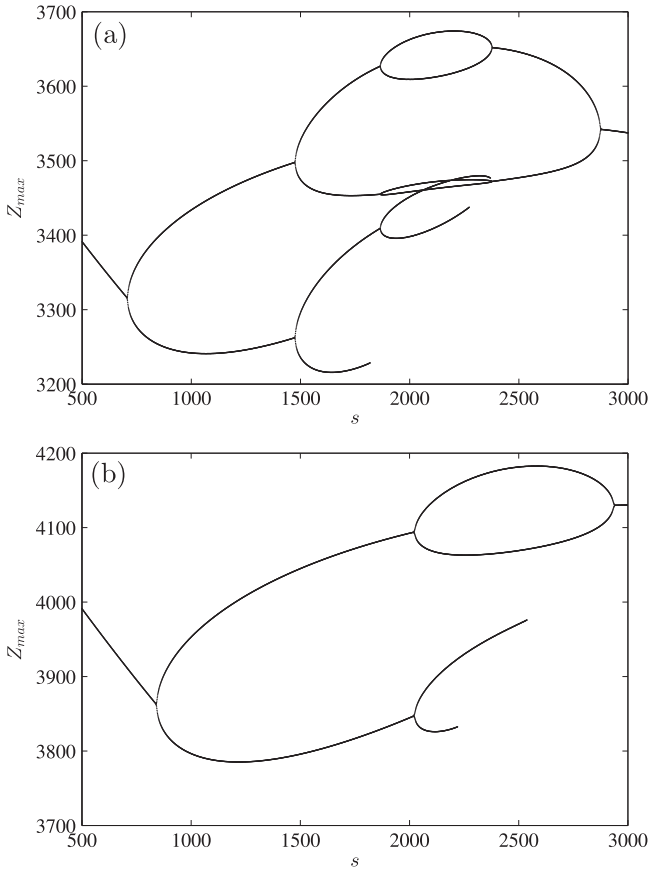

Figure 3. Bifurcation diagrams by plotting local maximum values $Z_{\max}$ in the range $500 \leqslant s \leqslant 3000$ at (a) $r = 2995$ and (b) $r = 3500$.

rescaled nonlinear equations:

$$\frac{\mathrm{d}x}{\mathrm{d}\tau} = y + \left(\frac{s}{r}\right)v + O(\epsilon), \tag{9}$$

$$\frac{\mathrm{d}y}{\mathrm{d}\tau} = -xz + O(\epsilon), \tag{10}$$

$$\frac{\mathrm{d}z}{\mathrm{d}\tau} = xy + O(\epsilon), \tag{11}$$

$$\frac{\mathrm{d}v}{\mathrm{d}\tau} = -x + O(\epsilon), \tag{12}$$

with scalings [7]:

$$\epsilon = \frac{1}{r^{1/2}},\ \alpha = \frac{1}{\epsilon},\ \beta = \zeta = \frac{1}{\sigma\epsilon^2},\ \delta = 1. \tag{13}$$

If the parameter s is fixed, the ratio $s_r = s/r$ becomes negligible for large r and we retain the same rescaled Lorenz equations derived in Sparrow [12] which leads to the result that solutions are periodic for large r [11–13]. If the parameter s is of order $O(r)$, then s_r becomes constant and non-zero. Including the ratio s_r, the equations (9)–(12) satisfy the following integral relations

$$y^2 + z^2 = B^2, \tag{14}$$

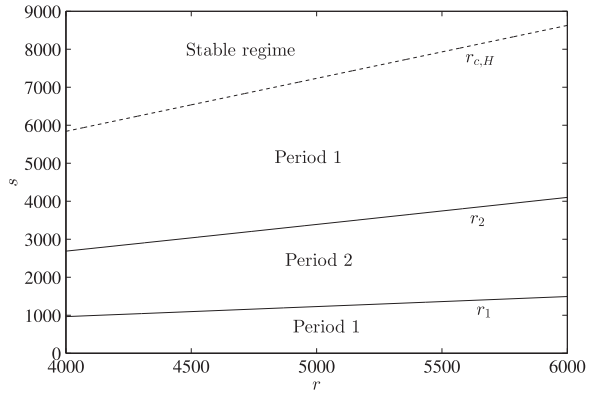

Figure 4. Regimes of fixed and periodic solutions divided by $r_{c,H}$, r_1 and r_2 for $4000 \leqslant r \leqslant 6000$.

$$z = \frac{1}{2}\left(x^2 + s_r v^2\right) + C, \tag{15}$$

or can be expressed in terms of an elliptic integral form as

$$\frac{\mathrm{d}z}{\mathrm{d}\tau} = \frac{x}{\sqrt{x^2 + s_r v^2}}\sqrt{2(z - C)(B + z)(B - z)}\,. \tag{16}$$

For non-zero $s_r > 0$, this elliptical integral (16) is not analytically solvable. However, these equations imply that the variable z lies on a circle of radius B for large r and $s_r \geqslant 0$, and it explains why the chaotic regime no longer exists for sufficiently large r and s in the Lorenz–Stenflo equations.

It is also noticeable that outside the chaotic regime, there are not only regimes of period 1 and doubled-period solutions but also wide regimes of period 3, 5 and 6 which are not observed in the Lorenz equations. But these wide periodic regimes are in fact well observed in other physical systems, for instance, nonlinear non-autonomous MLC circuit [14] or chaotic neural firing patterns in neuroscience [15]. Figure 3 displays bifurcation diagrams of $Z_{\max}$ around these regimes for fixed r. The forward bifurcations begin from period 1 as s increases and interestingly, instead of period doubling, bifurcations are disconnected before the backward bifurcations occur.

For $r > 3740$, only fixed, period 1 or 2 solutions exist. Figure 4 displays lines r_1 and r_2 which distinguish regimes of period 1 and 2, and the critical value $r_{c,H}$ for $4000 \leqslant r \leqslant 6000$. The lines r_1 and r_2 are obtained numerically. When the regression analysis is applied for this range of r, both lines r_1 and r_2 satisfy linear relationships as

$$r_1\colon\ s = 0.2639r - 91.919,\ R^2 = 1, \tag{17}$$

$$r_2\colon\ s = 0.7087r - 152.67,\ R^2 = 1, \tag{18}$$

where R^2 denotes the coefficient of determination. It is remarkable that for large r, there exist not only the period 1 regime if $0 \leqslant s_r < 0.2639$ or $0.7087 < s_r < 1/A_H = 1.391$,

but also the regime of period 2 solutions if $0.2639 < s_r < 0.7087$.

4. Conclusions

We investigated numerically periodic behaviors of the Lorenz–Stenflo equations in wide ranges of the parameters r and s. From the local maximum values of Z, the periodicity of solutions was computed and its diagram was obtained in the r–s parameter space. In regime of instability, both chaotic and periodic solutions exist and for sufficiently large r and s, the regime of chaotic solutions is enclosed by the regime of periodic solutions so that no chaotic solution exists for $r > 2975$ or for $s > 2340$. And inside the chaotic regime, there are regimes of the periodic solutions with complex patterns like periodic islands of a shrimp shape [7], long bands or thin curves with various periodicity. Moreover, there are regimes of periodic solutions with disconnected bifurcations outside the chaotic regime. This can be of interest in atmospheric turbulence research since it implies that very large-scale quasi-stationary orbits can appear and change their periodicity slowly for very large Rayleigh number and effect of rotation. However, we were not able to verify qualitatively why the chaotic regime is closed by period 1 and 2 regimes, nor able to predict quantitatively when the chaotic regime will be closed or when the regimes like long bands or shrimp-shape periodic islands appear which should be followed by future works.

Acknowledgments

This work was supported by the National Research Foundation of Korea (NRF) grant funded by the Korea Ministry of Science, ICT and Future Planning (MSIP) (No. 2011–0017041).

References

[1] Stenflo L 1996 *Phys. Scr.* **53** 83–84
[2] Lorenz E N 1963 *J. Atmos. Sci.* **20** 130–41
[3] Yu M Y and Yang B 1996 *Phys. Scr.* **54** 140–2
[4] Yu M Y, Zhou C T and Lai C H 1996 *Phys. Scr.* **54** 321–4
[5] Zhou C, Lai C H and Yu M Y 1997 *J. Math. Phys.* **38** 5225–39
[6] Zhou C, Lai C H and Yu M Y 1997 *Phys. Scr.* **55** 394–402
[7] Xavier J C and Rech P C 2010 *Int. J. Bifurcation Chaos* **20** 145–52
[8] Gallas J A C 1993 *Phys. Rev. Lett.* **70** 2714–7
[9] Bonatto C, Garreau J C and Gallas J A C 2005 *Phys. Rev. Lett.* **95** 143905
[10] Albuquerque H A, Rubinger R M and Rech P C 2008 *Phys. Lett.* A **372** 4793–8
[11] Dullin H R, Schmidt S, Richter P H and Grossmann S K 2007 *Int. J. Bifurcation Chaos* **17** 3013–33
[12] Sparrow C 1982 *The Lorenz Equations: Bifurcations, Chaos, and Strange Attractors* (Berlin: Springer)
[13] Robbins K A 1979 *SIAM J. Appl. Math.* **36** 457–71
[14] Thamilmaran K and Lakshmanan M 2002 *Int. J. Bifurcation Chaos* **12** 783–813
[15] Gu H and Xiao W 2014 *Int. J. Bifurcation Chaos* **24** 1450082